INVESTIGATION OF SINGLE CRYSTAL MICROWAVE ACOUSTICAL DELAY LINE MATERIALS

by

M. Kestigian, R. Kedzie, J. Worley, R. Damon
W. Croft and A. Smith

FINAL REPORT
Contract No. NAS 12–571
August 1968

Prepared for

ELECTRONICS RESEARCH CENTER
NATIONAL AERONAUTICS AND SPACE ADMINISTRATION
CAMBRIDGE, MASSACHUSETTS

by

SPERRY RAND RESEARCH CENTER
SUDBURY, MASSACHUSETTS 01776

SPERRY RAND RESEARCH CENTER
SUDBURY, MASSACHUSETTS 01776

SRRC–CR–68–39

INVESTIGATION OF SINGLE CRYSTAL MICROWAVE ACOUSTICAL DELAY LINE MATERIALS

by

M. Kestigian, R. Kedzie, J. Worley, R. Damon
W. Croft and A. Smith

FINAL REPORT

Contract No. NAS 12–571
August 1968

Prepared for

ELECTRONICS RESEARCH CENTER
NATIONAL AERONAUTICS AND SPACE ADMINISTRATION
CAMBRIDGE, MASSACHUSETTS

by

SPERRY RAND RESEARCH CENTER
SUDBURY, MASSACHUSETTS 01776

SPERRY RAND RESEARCH CENTER
SUDBURY, MASSACHUSETTS 01776

TABLE OF CONTENTS

LIST OF ILLUSTRATIONS

LIST OF ILLUSTRATIONS (cont.)

INVESTIGATION OF SINGLE CRYSTAL MICROWAVE ACOUSTICAL DELAY LINE MATERIALS

by

M. Kestigian, R. Kedzie, J. Worley, R. Damon
W. Croft and A. Smith

SECTION I

SUMMARY

Single crystal growth of $LiNbO_3$ and $LiTaO_3$ by the Czochralski method is described. Growth conditions are discussed in detail, and procedures for annealing and poling these crystals are also given. The effects of adding MgO to the melt are described too, since it was found that this innovation resulted in improved crystals.

Several measurement techniques for evaluating the quality of the grown crystals are described. Among these are measurements of the piezoelectric activity, optical measurements, and microwave acoustic attenuation measurements. Special emphasis is placed on the latter technique, as it is an extremely sensitive method of noting subtle differences between crystals of high quality. Measurements of the attenuation vs temperature at 2.7 GHz are presented for both pure and MgO-doped $LiTaO_3$ and $LiNbO_3$. These data indicate that the temperature-independent portion of the attenuation is reduced by MgO doping, thus indicating that doping results in the growth of more perfect crystals.

SECTION II

INTRODUCTION

A number of interesting and potentially useful new piezoelectric crystals have been synthesized recently. Among these are the materials lithium metatantalate ($LiTaO_3$) and lithium metaniobate ($LiNbO_3$), which have been chosen for this study. These materials have been found to exhibit extremely low attenuation (Refs. 1-5) of microwave acoustic waves. This property makes them very attractive for use in delay lines and acoustic signal processing devices operating at microwave frequencies. In addition, other authors (Refs. 6-16) have reported optical properties of these materials which make them well suited for many electro-optic and photoelastic applications. However, of particular interest in this study are the acoustic properties of these materials, since these properties are important to delay line applications (Ref. 17). These applications are of considerable importance because there is an increasing need for microwave acoustic devices that can provide real-time delay of microwave signals. Solid state delay lines operating at microwave frequencies can provide many advantages over conventional delay techniques, including lower loss and smaller size.

Because lithium niobate and lithium tantalate are both piezoelectric, they are well suited to acoustic applications where broadband devices are desired, since with piezoelectric materials resonant plates or thin films are not needed to generate the acoustic waves. Instead, a nonresonant process in which acoustic excitation (Refs. 18-20) takes place at the end surface of the rod, is used.

In this program, single crystals of both $LiNbO_3$ and $LiTaO_3$ have been grown. The Czochralski direct-melt crystal-growth technique was employed for growing both MgO-doped and undoped single crystals. The growth procedures and the methods for annealing and poling to obtain single-domain piezoelectric materials are described in some detail. Difference between the niobate and tantalate systems are discussed, with specific reference to controlling the problem of coloration, which is related to oxygen deficiencies in the melt.

The as-grown crystals were fabricated into rods and polished for evaluation as microwave acoustical delay line materials. Acoustic attenuation measurements were performed on both the doped and undoped samples. The temperature independent portion of the attenuation was observed to be lower in the MgO-doped samples than in the undoped samples. These results are discussed in terms of the scattering of acoustic waves by crystal imperfections and the influence MgO doping has on crystal quality.

SECTION III

DISCUSSION

A. CRYSTAL GROWTH AND POLING

1. $LiNbO_3$ and $LiTaO_3$

Lithium metatantalate and lithium metaniobate single crystals were grown from the direct melt by the Czochralski technique (Refs. 21,22), the most successful method of growing large, high quality single crystals. A schematic drawing of the crystal growth apparatus is shown in Fig. 1, and a picture of a typical boule is shown in Fig. 2. In this approach, a rotating crystal seed is lowered into a melt of appropriate composition and then slowly withdrawn through a temperature gradient. Rotation of the seed eliminates spurious nucleation and also helps provide vibration-free, uniform mechanical movement of the seed holder. The crucible acts as the heat source for the melt as it converts energy radiated from the rf coil into heat. (An alternate technique which has been used to grow some crystals of this type, uses resistive heating elements instead of the rf coil; however, the rf-coil setup is preferred because it provides a means of almost instantaneous temperature control. The rf coil method was used to grow all the crystals prepared under this contract.) The alumina insulation holds the heat within the cylinder, while the quartz shield is required because carbon is given off as the Li_2CO_3 in the melt calcines. The quartz shield prevents the carbon (and iridium when an iridium crucible is used) from passing through the porous alumina cylinder and depositing on the rf coil. One of the more important advantages of the Czochralski technique is that the crystal can be observed during the growth process and adjustments of growth conditions can be made. In addition, the crystal growth is fairly rapid, usually 0.125 to 1.0 inch per hour. An inherent disadvantage of all melt techniques is the possibility of container contamination, but in the Czochralski technique this problem is not as severe as in methods in which the crystal is actually formed within the container.

The materials used in the melt to grow $LiNbO_3$ were Li_2CO_3 and Nb_2O_5, while Li_2CO_3 and Ta_2O_5 were used to prepare $LiTaO_3$. The purity of the Li_2CO_3 was 99.999% and the purity of the Ta_2O_5 and Nb_2O_5 was 99.99%. The melt temperature was approximately 75°C higher than the melting point of the crystal being grown. In the case of $LiNbO_3$ the melt was held in a platinum crucible; an iridium crucible was used for $LiTaO_3$. It was found that the optimum withdrawal rate was about 0.25 inch per hour with a seed rotation rate of 20-26 rpm.

The most common method of obtaining colorless single crystals of $LiNbO_3$ is to grow them in an oxygen atmosphere. Oxygen prevents the formation of oxygen vacancies within the crystal lattice which give the crystal a light yellow or yellow-green color. An alternate method of producing colorless single crystals

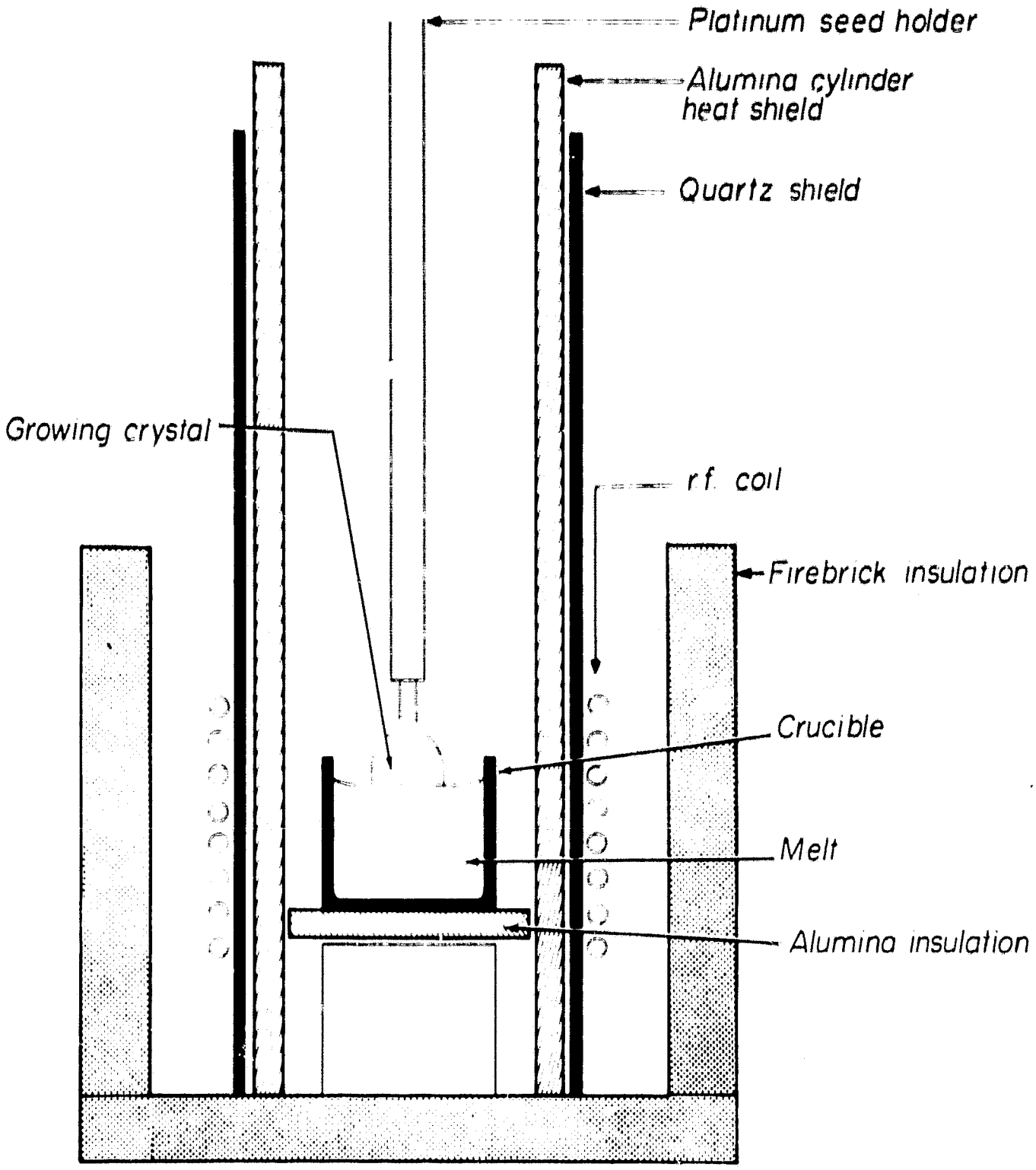

FIG. 1 Schematic diagram of Czochralski single crystal growth apparatus.

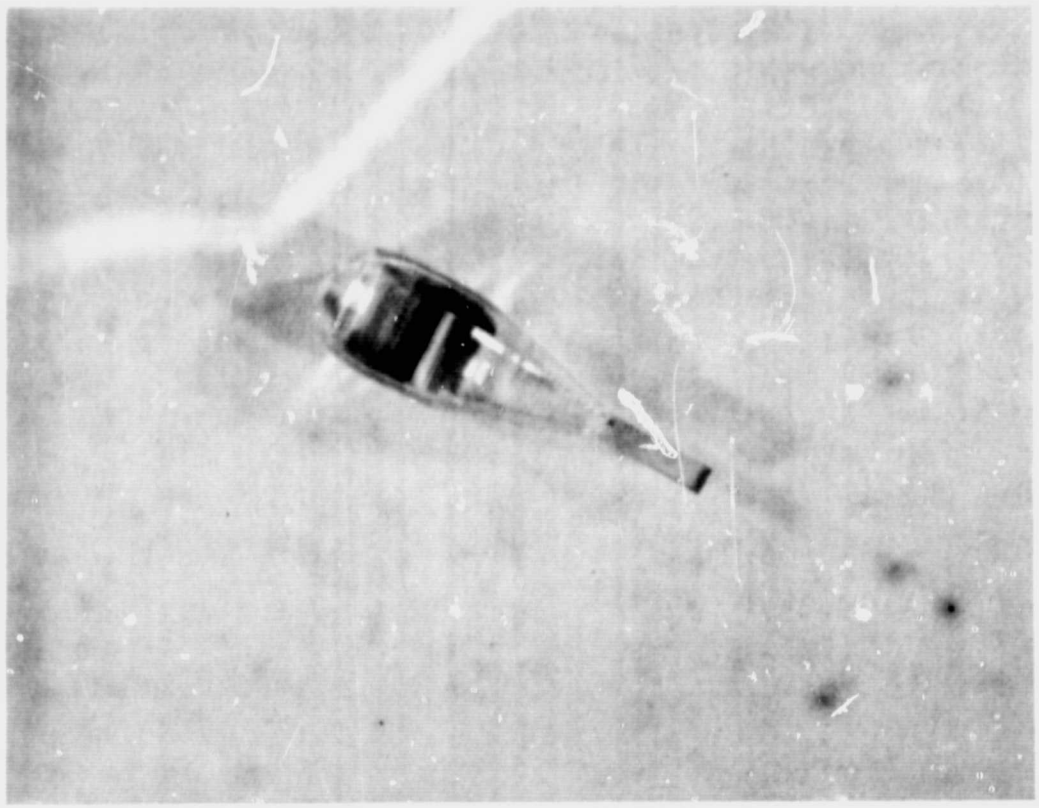

FIG. 2 Photograph of $LiNbO_3$ single crystal boule.

is to grow them in air under atmospheric conditions and then anneal them for twelve hours at 1000°C in an oxygen atmosphere. We found the latter method preferable since it produced crystals having less strain. In the case of $LiTaO_3$, we found that neither method produced completely colorless single crystals. Since both methods gave about the same amount of coloration, we chose to grow $LiTaO_3$ crystals in air under atmospheric conditions with subsequent anneal in oxygen, as with $LiNbO_3$.

In order to determine the nature of the coloration in $LiTaO_3$, various refinements in the growth process were tried. Container material was one of the first variables to be examined in this study. The high melting point of

$LiTaO_3$ (1670°C) precludes the use of pure platinum containers with an rf heat source because platinum melts at 1774°C. Although pure rhodium and platinum-rhodium alloy crucibles have been successfully used in the preparation of $LiTaO_3$ single crystals, the crystals have been of poorer optical quality than those normally obtained using iridium crucibles.

It has been shown that only a limited variation in composition (Refs. 23, 24) is possible for $LiNbO_3$ single crystals; however, this is not the case for the metatantalate system (Ref. 25). The stoichiometry of the $LiTaO_3$ melt plays a major role in the composition of the single crystal that is grown. Therefore, we have also examined the effect of melt stoichiometry in an effort to obtain higher quality $LiTaO_3$ single crystals. Crystals were grown from melts which contained as much as five mole percent excess of Ta_2O_5 or Li_2CO_3. It was found that the crystals grown from melts containing 5 mole percent excess Li_2CO_3 were slightly lighter colored than crystals grown from melts containing the same amount of excess Ta_2O_5. However, in neither case was it possible to obtain colorless crystals.

It is assumed that the coloration (light yellow-yellow green) of $LiTaO_3$ and $LiNbO_3$ prior to annealing is caused by thermal reduction of pentavalent tantalum or niobium with a corresponding charge-compensating deficiency of oxygen. $LiTaO_3$ and $LiNbO_3$ are of the form $A^{+1}B^{+5}O_3^{-6}$, where the A ion (lithium) has a valence of +1, and the B ion (Ta or Nb) has a valence of +5. However, Ta and Nb can also have a valence of +4. If $LiTaO_3$ or $LiNbO_3$ crystals grow with some of the Ta's or Nb's having this lower valence, then some of the oxygen lattice sites must be vacant in order to achieve charge balance. These oxygen vacancies cause the crystal to be colored and, as we will see later, also affect the acoustic attenuation of the crystal. Annealing in oxygen has been cited as one way to reduce the number of vacancies. Another way is to introduce a divalent cation in a concentration equal to the tetravalent Ta or Nb present; this should eliminate the oxygen vacancies, producing a colorless single crystal. Single crystals of $LiTaO_3$ and $LiNbO_3$ were therefore grown from melts which contained MgO as a minor constituent. The residual coloration was not completely eliminated from $LiTaO_3$ by this method, but the crystal quality was improved and the acoustic attenuation was reduced. No change in the coloration of $LiNbO_3$ was noted due to the addition of MgO to the melt, $LiNbO_3$ being normally colorless when prepared as described above. The effects of MgO doping are discussed in detail below.

The as-grown $LiNbO_3$ and $LiTaO_3$ single crystals exhibit a random arrangement of ferroelectric domains (Refs. 26, 27). Single-domain material has been obtained by three different methods (Refs. 26, 28). These are:

(a) addition of impurity oxides to the melt from which the crystal is grown;

(b) application of an electric field to the growing crystal;

(c) a two-step process in which the single crystal is grown and subsequently subjected to an electric field while being heated at a high temperature.

Techniques (b) and (c) have been shown to yield material of comparable high quality. However, the electric poling procedure, in which the single crystal is annealed, is more desirable because it also minimizes the thermal stresses that may cause the raw boule to fracture during the fabrication of samples.

The detailed poling procedure for $LiNbO_3$ is as follows. On a boule which is 2 to 3 cm long and 1 cm in diameter, a voltage of 0.6 V is applied and a current of about 2 mA flows at a temperature of 1190°C. Voltage and current are scaled appropriately for boules of different shapes. We found this temperature to be high enough for successful poling, although the published value (Ref. 29) of the Curie temperature is 1210°C. In early attempts to pole this material, higher voltages and currents were used (i.e., approximately 6 volts and 20 mA), but discoloration due to electrolytic reduction of the crystal was observed. This coloration can be removed without depoling by annealing the crystal at 1000 to 1100°C for about 12 hours in an oxygen atmosphere. However, by using the lower poling voltage mentioned above, electrolytic reduction is avoided and subsequent oxygen annealing is unnecessary.

A much higher voltage is required for poling $LiTaO_3$ crystals. About 700 V is used on a 2-3 cm long boule at a temperature of 700°C. A current of about 5 mA flows in a 1 cm diameter boule at this temperature. No objectionable discoloration due to electrolytic reduction results under these conditions. A much lower temperature can be used for this material than for $LiNbO_3$ because the Curie temperature of $LiTaO_3$ is only 665°C (Ref. 26). Prior to poling, $LiTaO_3$ crystals are annealed at 1000°C to 1100°C in an oxygen atmosphere for 12 hours to relieve any strains that might be present.

When poling grown crystals of $LiNbO_3$ or $LiTaO_3$, several different ways (Ref. 28) of making electrical connections to the boule may be employed. A "clothesline" configuration (i.e., the sample is suspended by the platinum wires used to make the electrical connections) is used for single crystals half an inch or less in diameter. Crystals of large diameter, on the other hand, are poled by a sandwich arrangement. In this procedure, flat ends are first cut and one end of the crystal is positioned upon a thin platinum-foil electrode in a furnace muffle. The second platinum electrode is held on the top of the single crystal by a refractory block.

2. MgO-Doped $LiNbO_3$ and $LiTaO_3$

In addition to the growth and evaluation of very pure $LiNbO_3$ and $LiTaO_3$ single crystals, we have also studied the effect of magnesium oxide additions, since magnesium ions could reduce the number of lattice vacancies in the manner discussed in the previous section. Doped $LiNbO_3$ single crystals were grown by the Czochralski process from melts which contained 0.01 and 0.02 mole percent MgO. These crystals were poled in the same manner as the undoped crystals.

$LiTaO_3$ single crystals with MgO doping were prepared from stoichiometric melts which contained 0.1, 0.2, and 0.3 mole percent MgO. Single crystals of MgO-doped lithium metatantalate were also grown from melts which contained up to five mole percent excess Li_2CO_3 and from melts with five mole percent excess Ta_2O_5.

Molybdenum oxide (MoO_3) doped $LiNbO_3$ single crystals have also been grown. The presence of molybdenum has been reported (Ref. 28) to yield single-domain $LiNbO_3$ single crystals. We found that the incorporation of molybdenum in $LiNbO_3$ invariably yielded a single crystal of poorer quality. The growth of MoO_3-doped $LiNbO_3$ single crystals was discontinued because the two other methods of obtaining single-domain single crystals were highly successful (see previous section).

A representative group of MgO-doped boules has been analyzed by emission spectroscopy. The results of the analysis of $LiTaO_3$ crystals are shown in the following table.

TABLE I

Analysis of $LiTaO_3$ Crystals

Mole % MgO added to melt	MgO present in crystal (ppm)		
	5% excess Li_2CO_3 in $LiTaO_3$	$LiTaO_3$	5% excess Ta_2O_5 in $LiTaO_3$
0.1	80		120
0.2	135	56	230

These data show that the crystals grown from MgO-doped melts which contained excess Ta_2O_5 had the highest magnesium content. This result was expected, since the magnesium is believed to go into the crystal structure on vacant lithium sites.

As may be seen in the following table, the magnesium content in MgO-doped $LiNbO_3$ is independent of the amount in the melt.

TABLE II

Analysis of $LiNbO_3$ Crystals

Mole % MgO added to melt	PPM MgO present in $LiNbO_3$ single crystal
0.01	74.5
0.02	75.0

The magnesium addition therefore seems to be entering the crystal only in the amount necessary to compensate a small fixed number of oxygen vacancies. This

result, however, contradicts the results of Nassau (Ref. 30), who found a smaller percentage of Mg in the grown crystal and observed that the amount in the crystal was proportional to that in the melt.

We found that MgO doping appears to lower the voltage which must be applied to pole $LiTaO_3$ crystals. Exhaustive data are not yet available, but it has been our experience that electric fields of 20 to 40 V/cm are sufficient to pole MgO-doped $LiTaO_3$, whereas a field of more than 100 V/cm is required for reliable poling of undoped samples. We also found that $LiTaO_3$ samples grown with excess Li_2O in the melt are much more difficult to pole than are samples that are stoichiometric or have excess Ta_2O_5. We do not presently understand the exact cause of this observed dependence of poling on composition.

B. CRYSTAL EVALUATION TECHNIQUES

In this section, we consider several methods of monitoring and comparing crystal quality. First, we describe methods of checking whether complete poling has been achieved. Next, optical inspection for strains is discussed. Finally, we will discuss comparisons between crystals made on the basis of microwave acoustic measurements.

1. Piezoelectricity Measurements

It is important for both the electro-optic and acoustic applications of $LiTaO_3$ and $LiNbO_3$ that a given sample constitute a single ferroelectric domain. A number of methods are available to determine whether the desired state has been successfully achieved by the poling procedure. In one technique (Ref. 27), the domain configuration is made visible under a microscope by etching or by polishing one side of the crystal. However, we have found it more convenient to employ a simple measurement of the piezoelectric constants. This measurement is made with the simple electrometer setup shown in Fig. 3. This method permits routine checking of all boules for the presence of a single domain prior to any fabrication.

In order to use this method, the ends of the crystal are cut flat so that electrodes can be applied as indicated. Usually the electrodes are bonded to c-axis faces which have been silver painted to ensure good electrical contact. With crystals of approximately ½-inch diameter, meter deflections of the order of 1 V are obtained with forces of the order of 1 kg. By use of this apparatus, the effective piezoelectric constant (Ref. 31), g, can be calculated from the meter reading by using the equation given in the figure. The value obtained for g using this circuit will be the same as the published value (Ref. 32) of this constant if the sample is completely poled. If the sample is incompletely poled, the contributions from different domains will tend to cancel, giving a lower meter reading, which indicates that the sample needs to be repoled.

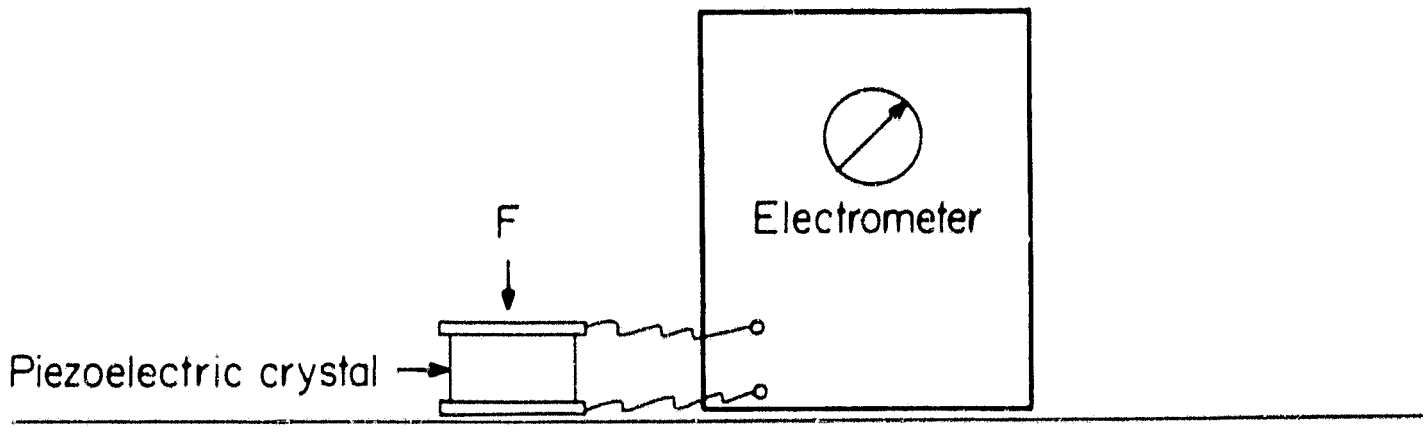

$$g = \frac{A}{F}\,\frac{V}{\ell}\,\frac{C_m + C_s}{C_s}$$

A, ℓ = sample area, length

C_s = sample capacity

C_m = meter capacity

V = meter reading

FIG. 3 Diagram of electrometer setup used for checking completeness of poling.

2. Optical Measurements

One of the standard methods of checking the quality of single crystal materials is to examine them under a polarizing microscope (Ref. 33). We have used this technique to examine polished oriented crystals of these materials in plane polarized light using both parallel and convergent illumination. The results of these measurements on typical crystals are as follows.

Good crystals of both $LiNbO_3$ and $LiTaO_3$ showed an absence of strain-induced birefringence when viewed down the [100] and [110] (hexagonal) directions. In certain crystals we observed incipient cleavage planes that could not be seen under ordinary illumination. These potentially fractured crystals could thus be eliminated by this type of examination. Viewed in parallel illumination down the [001] direction (c-axis), good $LiNbO_3$ crystals are uniformly bright (see Fig. 4a) during rotation of the crystal. On the other hand, even the best $LiTaO_3$ crystals usually show an irregular pattern of many extinction areas (see Fig. 4b). On a 4 mm thick slice, the interference colors (Ref. 33) vary between black and first-order gray, indicating a small variable birefringence which is too small to be measured by the usual Berek compensation techniques.

Both the niobate and tantalate are reported to crystallize with a rhombohedral unit cell (Refs. 34, 35) which would make them optically uniaxial. When conoscopically observed (Ref. 33) in convergent polarized light along the optical axis, $LiNbO_3$ gives a uniaxial interference figure with a large number of rings (Fig. 5) since it has a rather large birefringence (Ref. 6) ($n_e - n_o = -0.086$). The interference figure for $LiTaO_3$ is relatively simple (Figs. 6 and 7) because of its low birefringence ($n_e - n_o = +0.002$), but is very strain sensitive. Most $LiTaO_3$ crystals show a biaxial figure over part of the observed area. Scanning over a $LiTaO_3$ crystal in conoscopic observation, the isogyres are seen to separate in many areas by an amount corresponding to an angle between the two optic axes of up to several degrees. Since all $LiTaO_3$ crystals show these optical variations to a certain degree, these measurements provide a sensitive method for comparing relative amounts of strain in different crystals.

We have also tested the optical quality of our lithium niobate and lithium tantalate by inserting fabricated crystals into one arm of an interferometer. All crystals tested had been fabricated into rectangular parallepipeds 2.5 x 2.5 x 8 mm long for acoustic measurements. The ends were polished flat and mutually parallel. The Mach–Zehnder interferometer, shown in Fig. 8, provides a simple and convenient means of testing such samples. Photographs of the resulting fringe patterns are shown for a $LiNbO_3$ sample and a $LiTaO_3$ sample in Figs. 9a and 9b, respectively. These figures shown that strain-induced optical distortions in these crystals are so small that displacements of only a half fringe or less result. Many of the boules recently grown and all of the crystals used for acoustic measurements are of this level of optical quality. For comparison, Fig. 9c shows a fringe pattern produced by a poor quality YAG crystal of similar dimensions. This sample exhibits distortions which can be characterized by a displacement of approximately 20 fringes.

This interferometric technique does not yield direct information as to whether or not the crystals are single-domain. This is to be expected, since

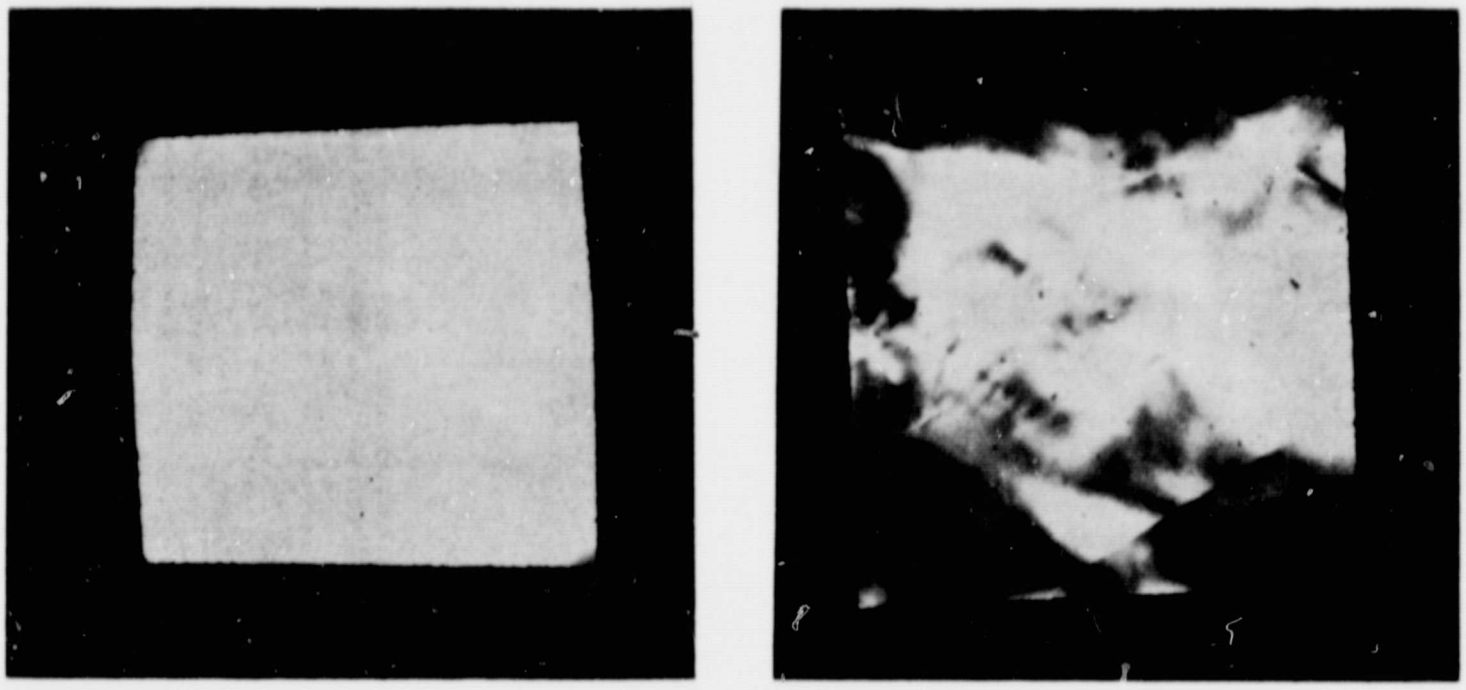

(a) (b)

FIG. 4 Views along the c-axis of $LiNbO_3$ (a) and $LiTaO_3$ (b) obtained using crossed polarizers and parallel illumination. (Sample cross section: 3 x 3 mm; sample thickness: 4 mm.)

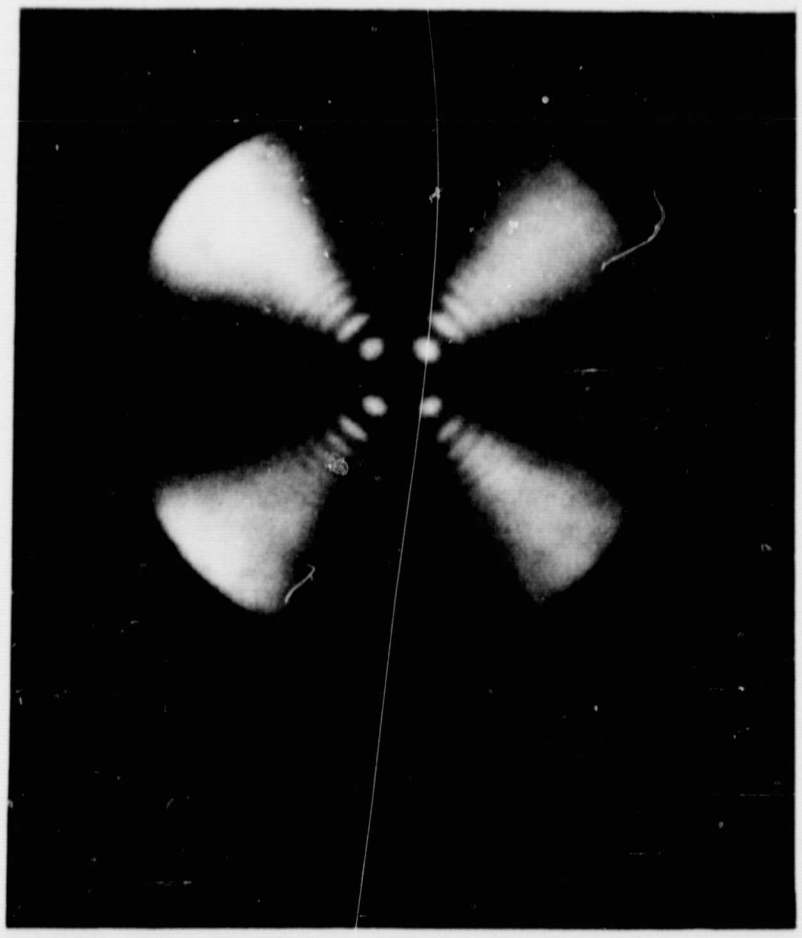

FIG. 5 Conoscopic image obtained by viewing $LiNbO_3$ in convergent polarized light. (1 mm thick sample viewed parallel to the c axis.)

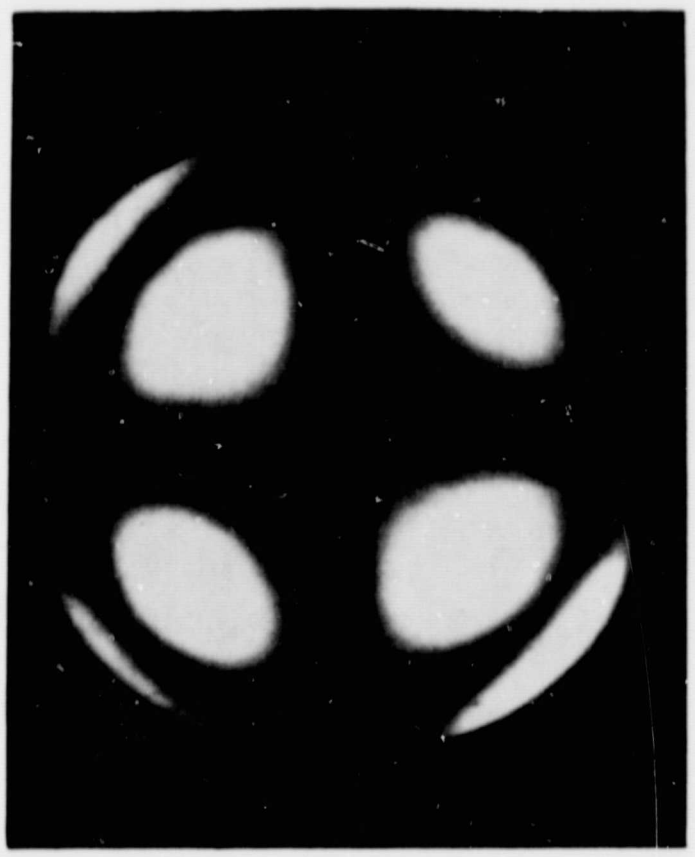

FIG. 6 Conoscopic image obtained by viewing $LiTaO_3$ in convergent polarized light. (1 mm thick sample viewed parallel to the c axis.)

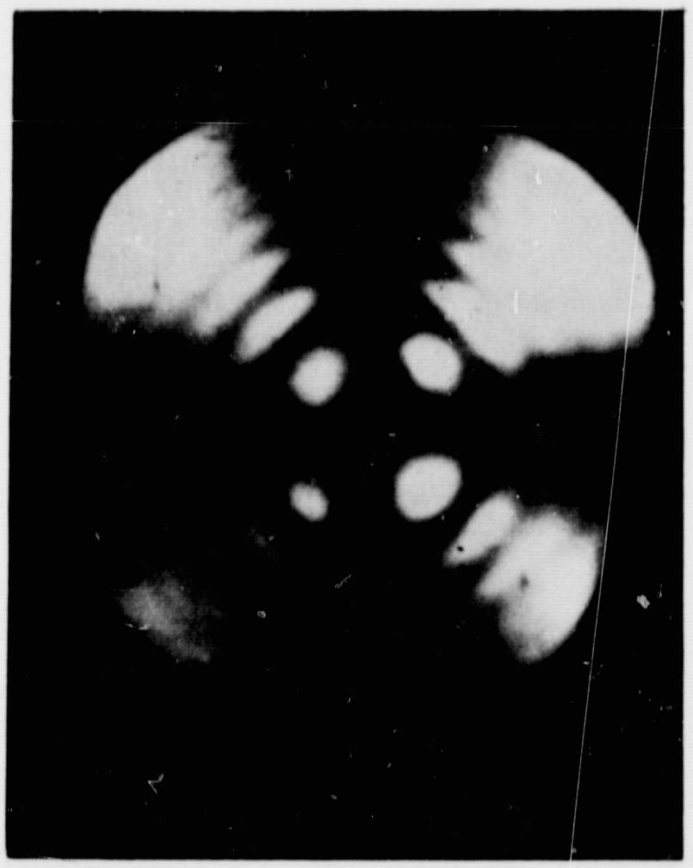

FIG. 7 Conoscopic image obtained by viewing $LiTaO_3$ in convergent polarized light. (4 mm thick sample viewed parallel to the c axis.)

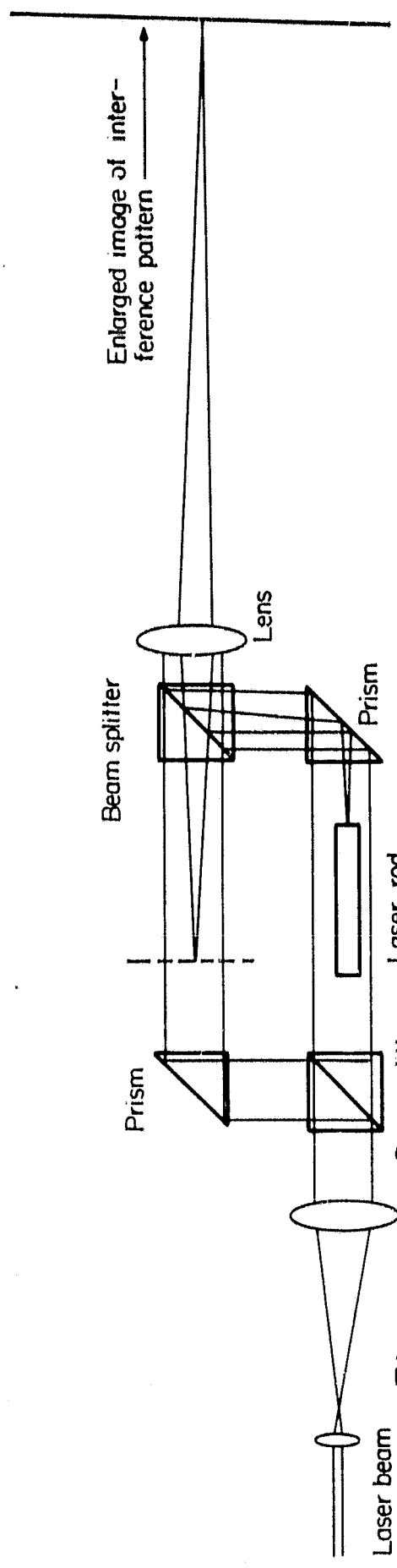

FIG. 8 Schematic diagram of Mach-Zehnder interferometer used to check optical quality of single crystal materials.

(a)

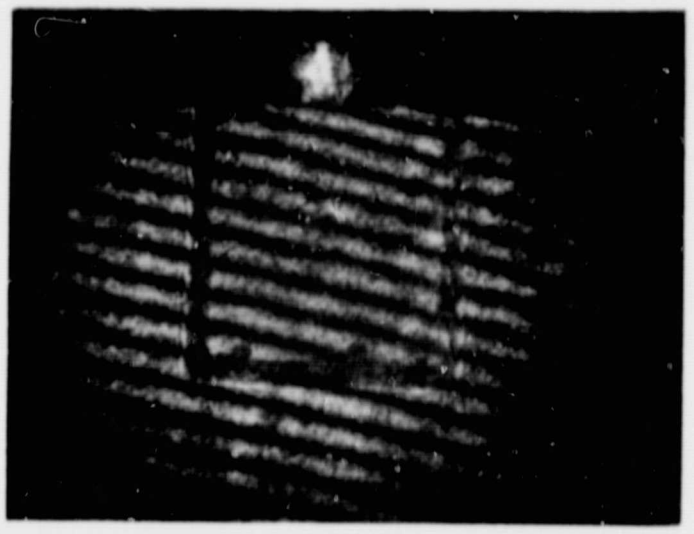

$LiTaO_3$

(b)

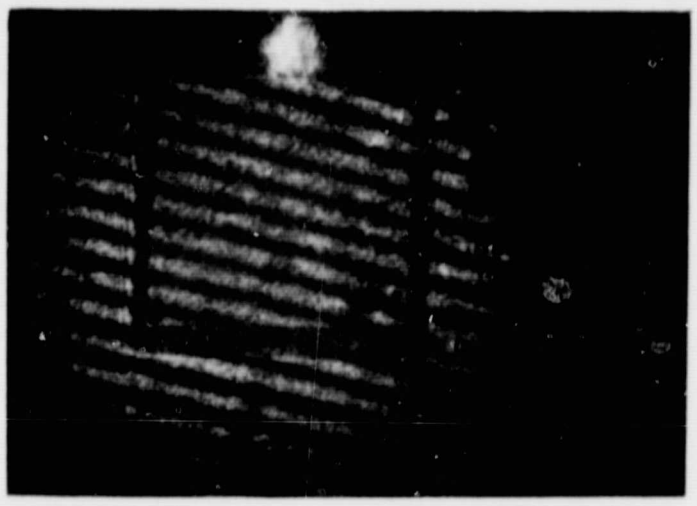

$LiNbO_3$

(c)

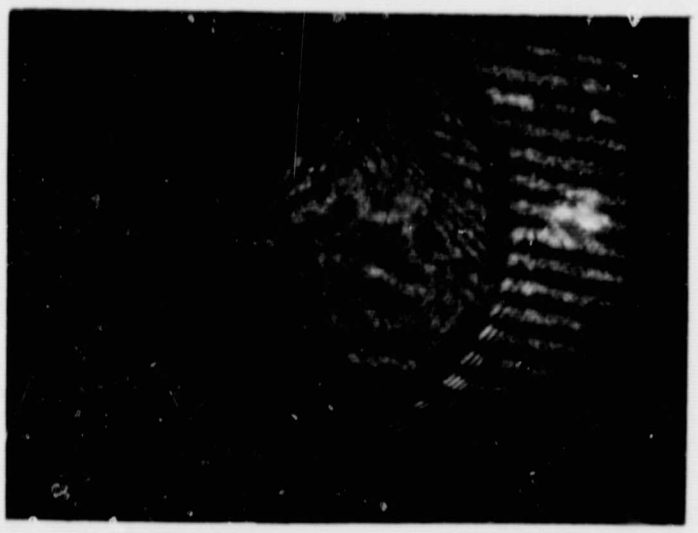

YAG

FIG. 9 Interference patterns obtained with the Mach-Zehnder interferometer in (a) a $LiTaO_3$ crystal; (b) a $LiNbO_3$ crystal; (c) a badly-strained YAG crystal.

the index of refraction does not change when the direction of domain polarization is reversed by 180 degrees. Any change of index within the domain walls themselves would probably not be noted with this technique because sufficient magnification of the image was not provided. Since more direct methods of checking for incomplete poling are available (see above), it was not felt necessary to adapt this technique to domain studies.

It should also be noted that our interferometer measurements have been made only on c-axis crystals. It has been reported (Ref. 36) that interferometer inspection along the "a" axis can be used to reveal very small variations in the optical refractive index which occur due to very small changes in chemical composition in the growth direction (i.e., along the "c" axis). Another technique (Ref. 16) for viewing these small index gradients along the "c" axis is by using crossed polarizers.

3. Acoustic Measurements

The electrometer and optical checks described above are useful for detecting gross defects such as incomplete poling or the presence of large strains. For detecting more subtle degrees of crystal quality, however, other methods are required. The measurement of acoustic attenuation is one very useful method of comparing crystals, since the attenuation rate is very sensitive to certain crystal imperfections. Because of this and because these materials are often used for acoustic applications, it seemed appropriate to make the series of attenuations measurements described below.

The ultrasonic attenuation α observed in single crystal materials (Ref. 37) may be categorized by two terms:

$$\alpha = A + Bf(T)$$

where A and B are constants for a given material and f(T) approaches zero at $T=0$. During the growth of a single crystal material, crystal imperfections may develop which contribute to the temperature independent acoustic attenuation represented by the first term. These defects may take the form of impurities, strains, or lattice site vacancies; they lead to a scattering of the acoustic waves such that there is a net loss of energy. The temperature dependent second term results from the interaction of acoustic waves with the thermal lattice vibrations. This term may be changed by the addition of impurities to the melt from which the crystal is grown, since there now would be different masses at some of the lattice sites. In our present work we were primarily interested, however, in lowering the temperature independent part of the attenuation by improving the quality of the crystal.

Figure 10 shows a schematic diagram of the 9.0 GHz pulse apparatus used for measuring acoustic attenuation. A 9.0 GHz magnetron triggered by a pulse modulator transmits rf energy through an attenuator, circulator, and tuner to the rod-shaped sample, one end of which is placed in the strong rf electric field of a microwave reentrant cavity. The sound wave pulse travels from the generating point at one end of the rod to the other end surface, where it is

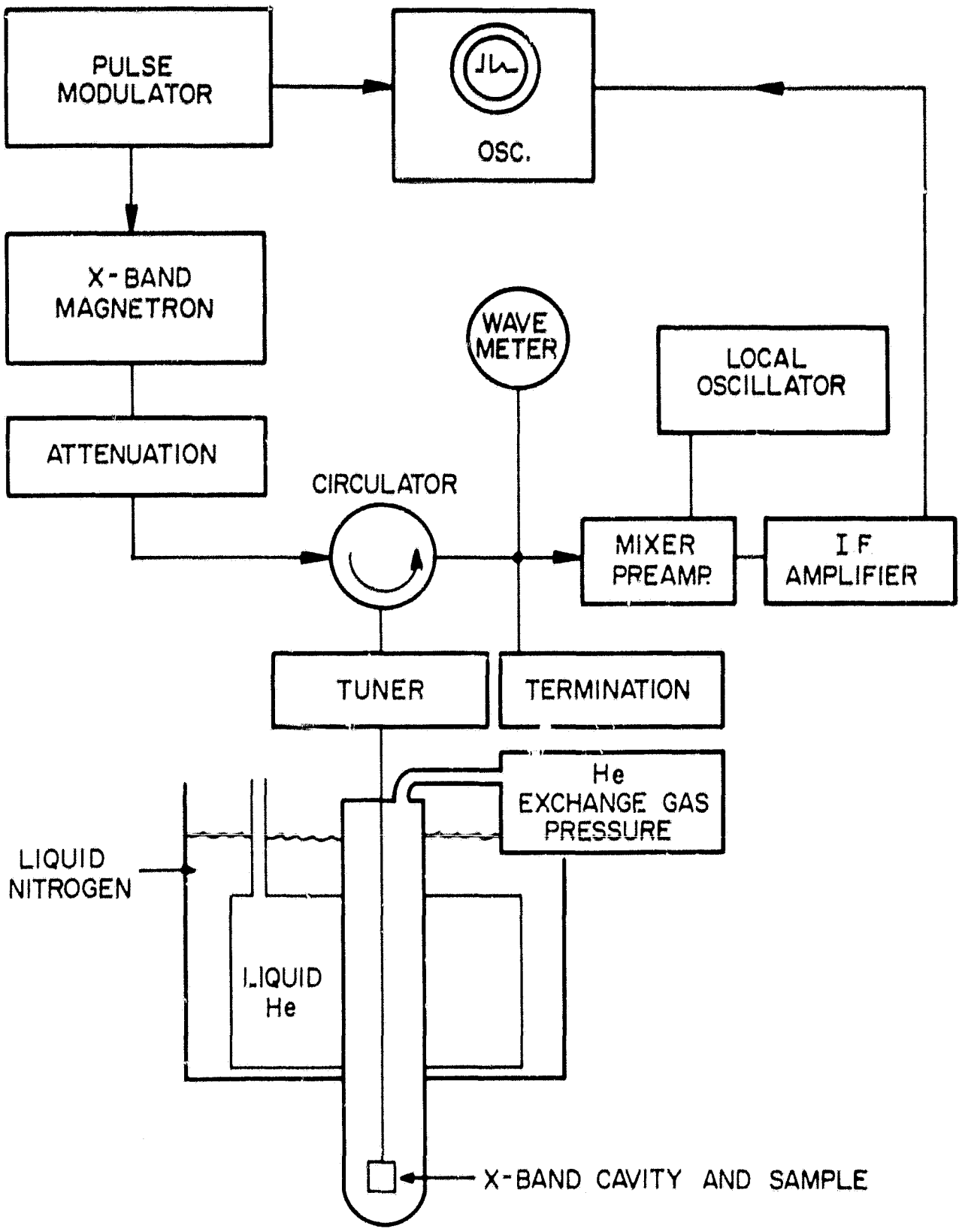

FIG. 10 Schematic diagram of the 9 GHz pulse apparatus for measuring acoustic attenuation as a function of temperature.

reflected. After retracing its path to the generating point, a portion of the sound wave is reconverted to electromagnetic energy and is coupled out of the cavity through the circulator to a mixer preamplifier. The intermediate frequency, obtained by beating the signal from the cavity with the output of a local oscillator, is amplified, detected, and displayed on an oscilloscope. The attenuation measurements are made by a pulse-echo technique which consists of comparing the amplitude of the first echo with subsequent echoes.

a. Lithium Metaniobate. Figure 11 shows the attenuation of longitudinal acoustic waves measured in $LiNbO_3$ as a function of temperature. The upper curve represents the lowest attenuation data obtained from measuring several samples without MgO. The lower curve shows the results obtained with a doped sample. The difference between these two curves is typical of the differences we have noted between doped and undoped samples. That is, the attenuation at very low temperatures is decreased, but the general shape of the attenuation vs temperature characteristic is not altered. This would lead one to believe that the addition of MgO to the melt has resulted in a more perfect crystal because crystal perfection determines the attenuation at very low temperatures. In general, crystal imperfections are the only mechanism which can scatter the acoustic beam at low temperatures, since interactions with thermal phonons only become important at higher temperatures. This can be seen by the rise in the attenuation data above 40°K. These interactions with thermal phonons are not appreciably affected by MgO additions, indicating, as expected, that the addition of MgO does not make gross changes in the phonon modes of the crystal.

The results of shear-wave studies at 8.5 GHz for a doped and the best undoped sample are shown in Fig. 12. The attenuation at low temperatures is approximately 20% lower in the MgO-doped sample. Although this change is small, we are convinced that the difference is real. A slight change in the slope can also be seen in this figure.

It should be stressed in connection with these last figures that the measured value of attenuation can be affected by sample dependent variables, such as nonparallelism or lack of flatness of end faces, as well as by the properties of the material itself. However, careful sample preparation and the occurence of the same behavior with several other samples leads us to believe that the results shown in these figures represent real differences between the properties of doped and undoped $LiNbO_3$ crystals.

In addition to the X-band measurements described above, we have also made measurements of the longitudinal-wave attenuation in $LiNbO_3$ at 2.75 GHz. At this frequency, the attenuation is low enough to make measurements over the entire 4-300°K temperature range. The results of such measurements on doped and undoped crystals are shown in Fig. 13. Here we have subtracted the 4°K value of attenuation from each curve before plotting, so that we can compare the temperature dependent portions of the attenuation. These curves show a slightly lower attenuation in the doped crystal. Further measurements on other samples will be required to determine whether this difference is significant.

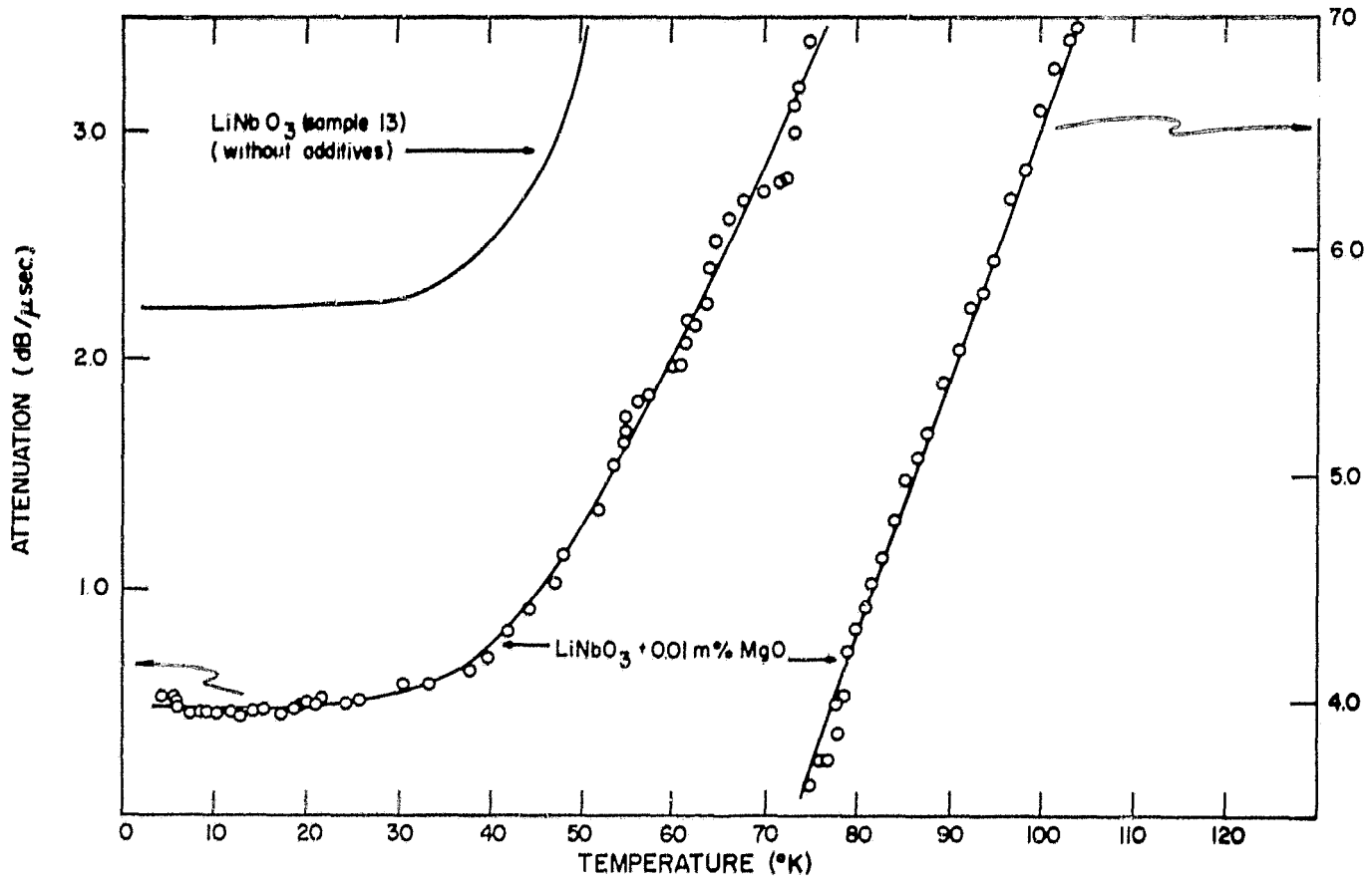

FIG. 11 Longitudinal acoustic-wave attenuation in two samples of c-axis oriented $LiNbO_3$ as a function of temperature at X-band frequencies. The upper solid curve is due to $LiNbO_3$ without added impurities, and the other curves drawn through the open circles are due to $LiNbO_3$ doped with 0.01 mole % MgO. Two separate ordinates are used for the data on the doped crystals.

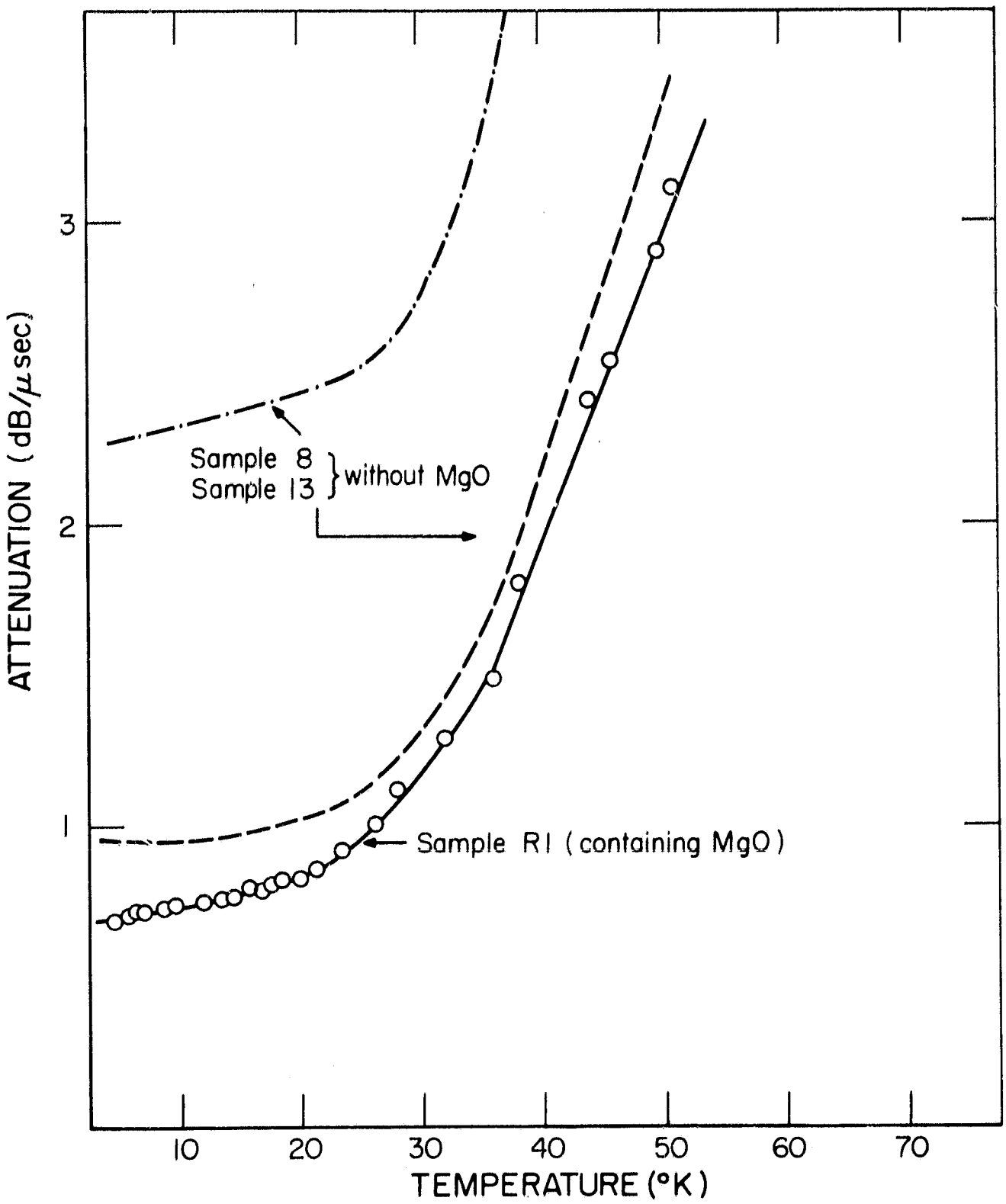

FIG. 12 Temperature-dependent attenuation of shear elastic waves compared at X-band frequencies for MgO-doped and undoped $LiNbO_3$ single crystal rods. The broken curves are drawn through the data points obtained for two undoped crystals. The open circles are the data points obtained from a $LiNbO_3$ single crystal rod doped with 0.01 mole % MgO.

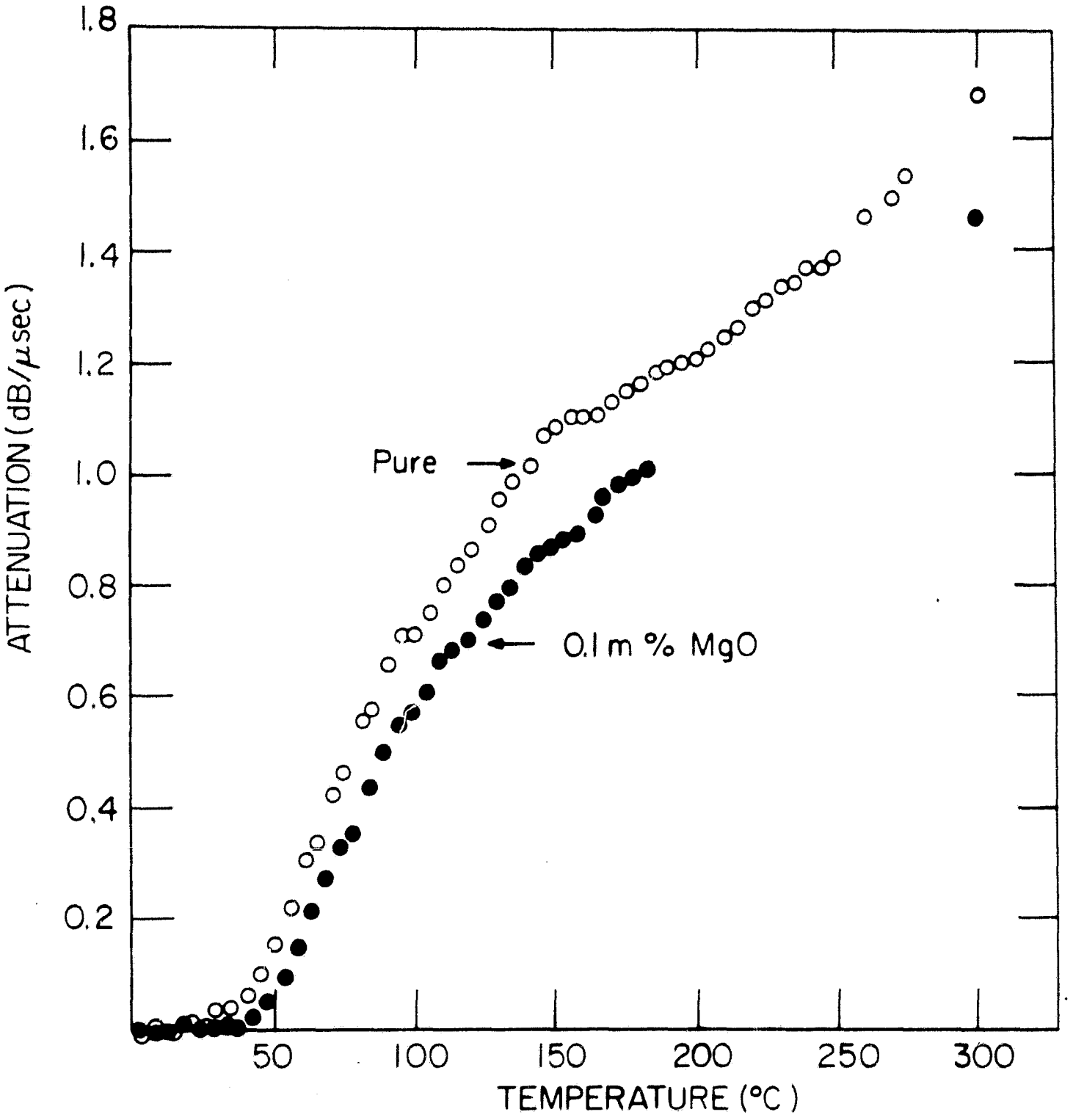

FIG. 13 Longitudinal-wave attenuation vs temperature for pure and MgO-doped $LiNbO_3$ at 2.75 GHz. (The temperature-independent portion of the attenuation has been subtracted from both of these curves.)

b. Lithium Metatantalate. Acoustic attenuation measurements were also performed on single crystals of $LiTaO_3$ suitably fabricated for microwave transmission experiments. The results of longitudinal acoustic wave generation in several single crystal rods are compared in Fig. 14. The solid lines were drawn through data obtained from single crystals grown without additives. The open circles are the data points obtained for $LiTaO_3$ doped with 0.1 mole percent MgO and 5 mole percent excess of Ta_2O_5. Note that although a much smaller temperature-independent attenuation region exists at low temperatures the attenuation between 4^oK and 18^oK is less than the better sample without additives. Several other interesting features of the data are readily apparent. The rate of increase in attenuation with increasing temperature is more rapid for the MgO-doped sample than it is for the undoped samples. This seems to indicate a shift in the thermal phonon distribution which produces a greater interaction with the sound waves. In addition, a sharp reduction in the attenuation rate occurs for both the doped and undoped samples between 35^oK and 58^oK. This effect may be related to a similar plateau in lower frequency measurements, discussed below, but more work will be required before its origin is known for certain. The reduction in the temperature-independent attenuation has allowed us to observe a single longitudinal echo at room temperature for the first time at X-band frequencies.

As with the $LiNbO_3$ samples, another $LiTaO_3$ sample was studied at liquid helium temperatures to confirm that the lower attenuation in the doped sample was not due to sample dependent effects. This second sample gave similar results.

Previous attempts to generate shear-wave echoes in undoped $LiTaO_3$ at X band were unsuccessful. The improvement in crystal quality achieved by the addition of MgO has now allowed us to make the first X-band temperature dependence measurements of shear-wave attenuation in $LiTaO_3$. The results of this experiment are shown in Fig. 15. Note that a region of temperature-independent attenuation does not exist, and a very rapid rise in attenuation occurs at relatively low temperatures. This behavior is similar to that observed in $LiNbO_3$ (Ref. 2).

As with $LiNbO_3$, we also measured the longitudinal-wave attenuation of $LiTaO_3$ at 2.75 GHz. The results are plotted in Fig. 16. In contrast to the $LiNbO_3$ data, these preliminary results show that the temperature-dependent portion of the attenuation is larger in the MgO-doped crystal. However, if both the temperature dependent and independent terms are considered, the total room temperature attenuation is about the same in these two samples. The plateau at $\approx 50^oK$ that is evident in this figure seems to be related to the presence of reduced tantalum ions. This conclusion is indicated by preliminary measurements on a number of $LiTaO_3$ crystals with different stoichiometries. These latter measurements are being made at the Sperry Rand Research Center under a program supported in part by Wright-Patterson Air Force Base under Contract No. F33615-68-C-1099.

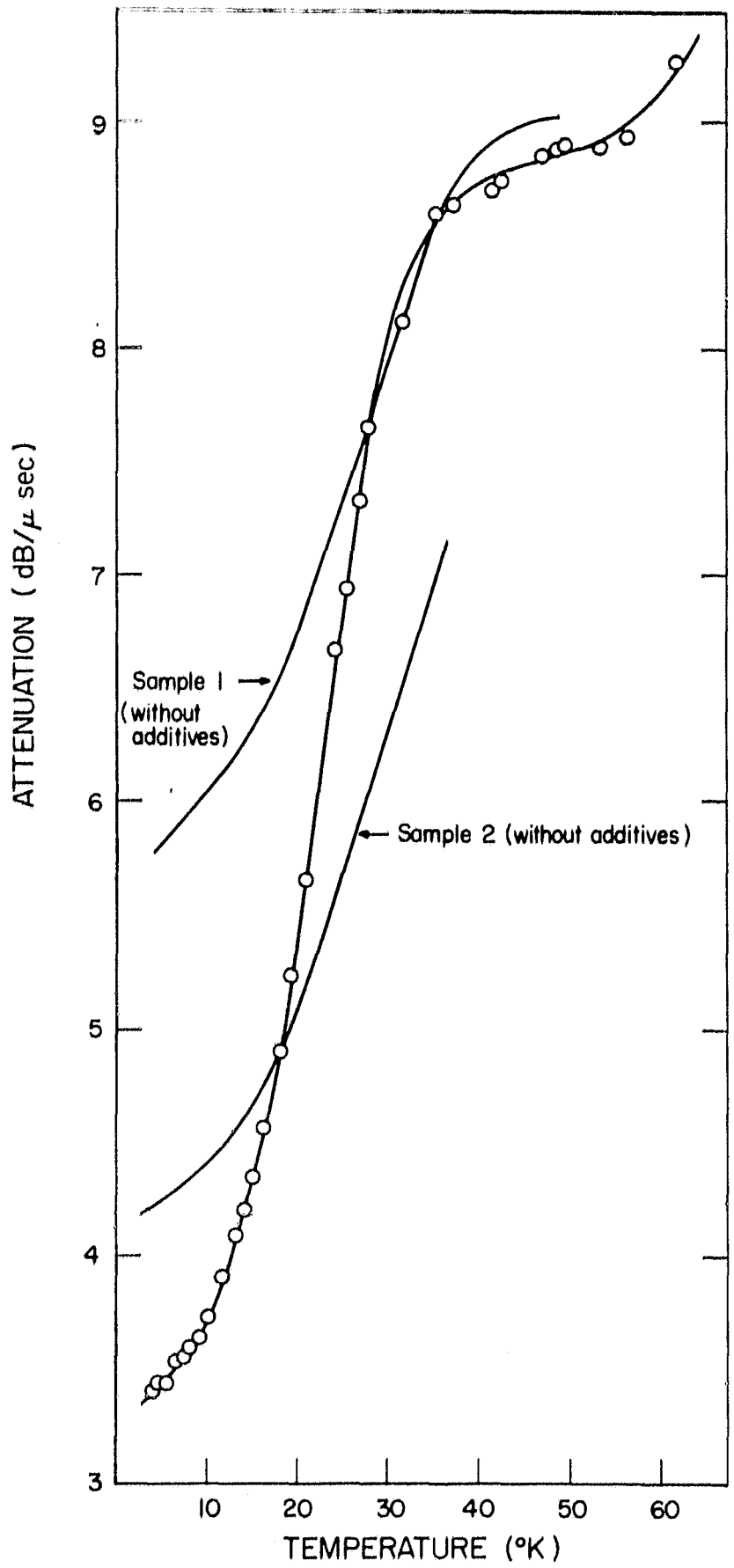

FIG. 14 Temperature-dependent longitudinal acoustic-wave attenuation in c-axis oriented $LiTaO_3$ rods at X-band frequencies. The solid curves are due to the attenuation of single crystals of $LiTaO_3$ grown without additives. The open circles are the data points obtained for $LiTaO_3$ doped with 0.1 mole % MgO and a 5 mole % excess of Ta_2O_5.

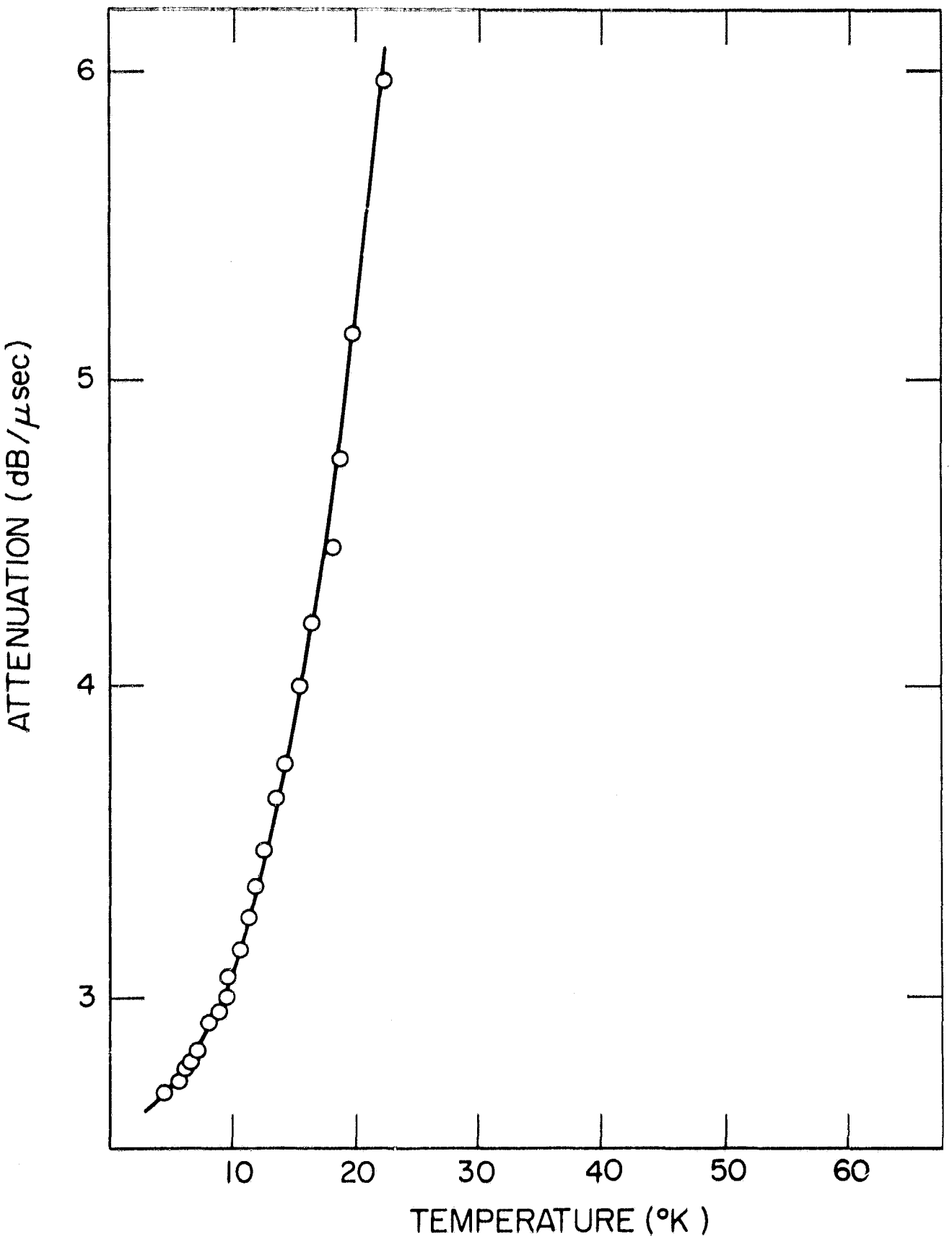

FIG. 15 Temperature-dependent shear-wave attenuation in a c-axis oriented $LiTaO_3$ single crystalline rod doped with 0.1 mole % MgO and a 5 mole % excess of Ta_2O_5.

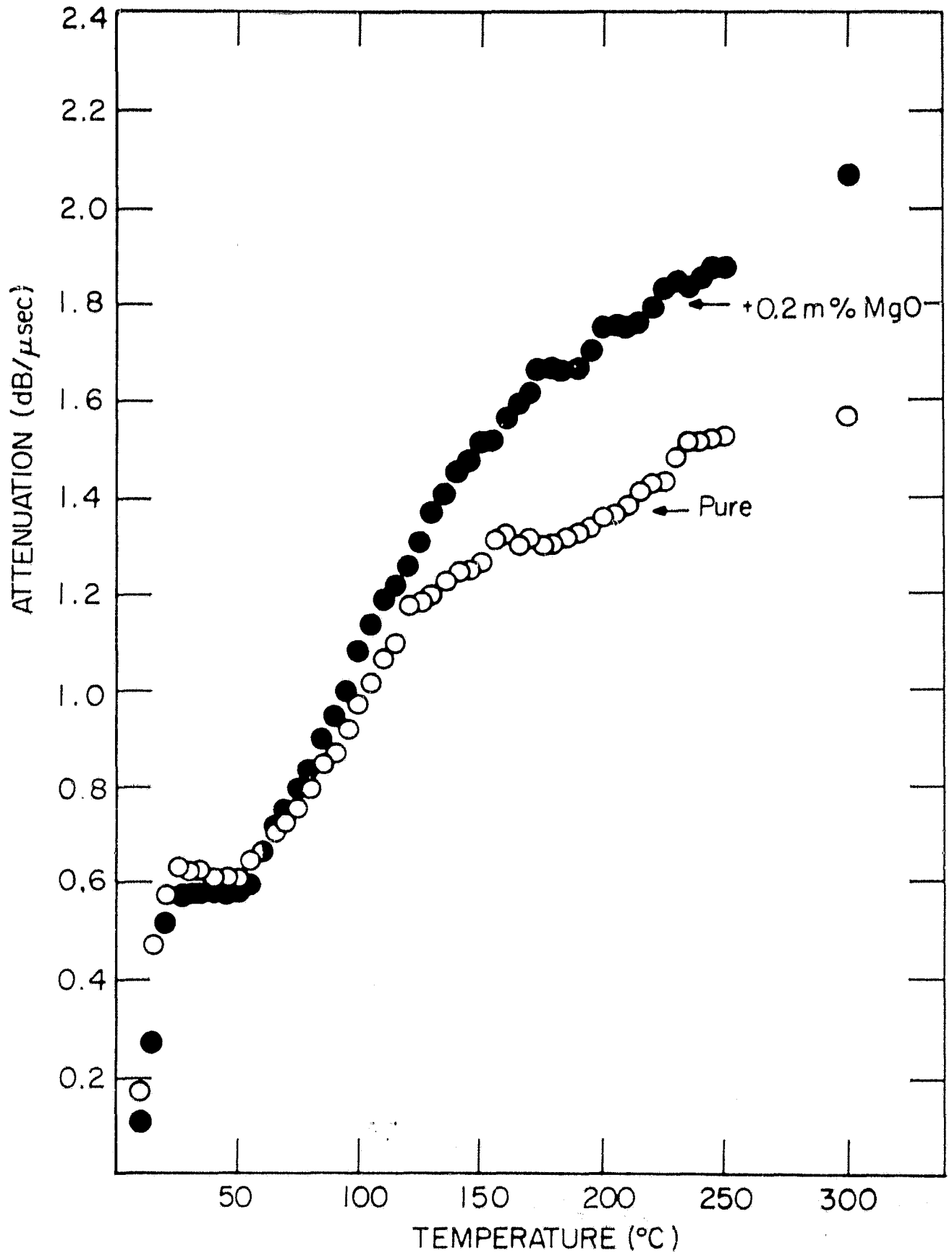

FIG. 16 Longitudinal-wave attenuation vs temperature for pure and MgO-doped $LiTaO_3$ at 2.75 GHz. (Both the doped and undoped crystals were grown from melts containing 5 mole % excess Li_2O. The temperature-independent portion of the attenuation has been subtracted from both of these curves.)

SECTION IV

CONCLUSIONS

Single crystals of $LiTaO_3$ and $LiNbO_3$ have been grown and evaluated, and procedures for annealing and poling these crystals have been developed. The growth experiments on these crystals were designed to optimize crystal quality by closely correlating changes in growth conditions with the results of measurements on the grown crystals. These measurements included measurements of the piezoelectricity of the crystal, optical measurements, and microwave acoustic attenuation measurements. Special emphasis was placed on the latter, since these measurements reveal suble differences between crystals which are not evident in the other methods. The emphasis on acoustic measurements is also appropriate because of the frequent use of these materials in microwave acoustic devices.

In the course of growing and evaluating $LiNbO_3$ and $LiTaO_3$ crystals, we have discovered that a significant improvement in crystal quality can be obtained by adding MgO to the crystal melt. We found that the temperature-independent portion of the microwave acoustic attenuation was reduced by such additions. We tentatively attribute this improvement to the presence of oxygen vacancies in the undoped material. These vacancies occur because of niobium or tantalum ions existing in a reduced valence condition in the doped material. Adding magnesium, which enters the structure on a lithium site, makes it possible for oxygen to occupy all the appropriate sites, resulting in a more perfect crystal.

SECTION V

REFERENCES

1. M. I. Grace, R. W. Kedzie, M. Kestigian and A. B. Smith, Appl. Phys. Letters 9, 155 (1966).

2. A. B. Smith, M. Kestigian, R. W. Kedzie and M. I. Grace, J. Appl. Phys. 38, 4928 (1967).

3. E. G. Spencer, P. V. Lenzo and K. Nassau, Appl. Phys. Letters 7, 67 (1965).

4. E. G. Spencer and P. V. Lenzo, J. Appl. Phys. 38, 423 (1967).

5. C. P. Wen and R. F. Mayo, Appl. Phys. Letters 9, 135 (1966).

6. E. G. Spencer, P. V. Lenzo and A. A. Ballman, Proc. IEEE 55, 2074 (1967).

7. P. V. Lenzo, E. G. Spencer and K. Nassau, J. Opt. Soc. Am. 56, 633 (1966).

8. P. V. Lenzo, E. H. Turner, E. G. Spencer and A. A. Ballman, Appl. Phys. Letters 8, 81 (1966).

9. E. H. Turner, Appl. Phys. Letters 8, 303 (1966).

10. G. E. Peterson, A. A. Ballman, P. V. Lenzo and P. M. Bridenbaugh, Appl. Phys. Letters 5, 62 (1964).

11. R. W. Dixon, J. Appl. Phys. 38, 5149 (1967).

12. E. G. Spencer, P. V. Lenzo, K. Nassau, IEEE Journal of Quantum Electronics QE-2, 69 (1966).

13. J. A. Giordmaine and R. C. Miller, Phys. Rev. Letters 14, 973 (1965).

14. G. D. Boyd, R. C. Miller, K. Nassau, W. L. Bond and A. Savage, Appl. Phys. Letters 5, 234 (1964).

15. J. E. Midwinter, Appl. Phys. Letters 12, 68 (1968).

16. J. E. Midwinter, J. Appl. Phys. 39, 3033 (1968).

17. R. W. Damon, IEEE Spectrum 4, 87 (June 1967).

18. H. E. Bömmel and K. Dransfeld, Phys. Rev. 117, 1245 (1960).

19. E. H. Jacobsen, J. Acoust. Soc. Am. 32, 949 (1960).

20. W. H. Haydl, K. Blötekjaer and C. F. Quate, J. Acoust. Soc. Am. 36, 1670 (1964).

21. S. A. Fedulov, Z. I. Shapiro, P. B. Ladyzhinskii, Soviet Physics — Crystallography 10, 218 (1965).

22. A. A. Ballman, J. Am. Ceram. Soc. 48, 112 (1965).

23. H. Fay, W. J. Alford and H. M. Dess, Appl. Phys. Letters 12, 89 (1968).

24. J. G. Bergman, A. Ashkin, A. A. Ballman, J. M. Dziedric, H. J. Levinstein and R. G. Smith, Appl. Phys. Letters 12, 92 (1968).

25. A. A. Ballman, H. J. Levinstein, C. D. Capio and H. Brown, J. Am. Ceram. Soc. 50, 657 (1967).

26. H. J. Levinstein, A. A. Ballman, C. D. Capio, J. Appl. Phys. 37, 4585 (1966).

27. K. Nassau, H. J. Levinstein and G. M. Loiacono, J. Phys. Chem. Solids 27, 983 (1966).

28. K. Nassau, H. J. Levinstein and G. M. Loiacono, J. Phys. Chem. Solids 27, 989 (1966).

29. K. Nassau, H. J. Levinstein, G. M. Loiacono, J. Phys. Chem. Solids 27, 983 (1966).

30. K. Nassau in Ferroelectricity (Elsevier Publishing Company, Amsterdam, 1967), E. F. Weller, ed., p. 259.

31. IRE Standards on Piezoelectric Crystals, Proc. IRE 37, 1378 (1949).

32. A. W. Warner, M. Onoe and G. A. Coquin, J. Acoust. Soc. Am. 42, 1223 (1966).

33. E. E. Wahlstrom, Optical Crystallography, John Wiley & Sons, Inc., New York, 1960.

34. S. C. Abrahams, J. M. Reddy and J. L. Bernstein, J. Phys. Chem. Solids 27, 997 (1966).

35. S. C. Abrahams and J. L. Bernstein, J. Phys. Chem. Solids 28, 1685 (1967).

36. J. E. Midwinter, Appl. Phys. Letters 11, 128 (1967).

37. M. Pomerantz, Proc. IEEE 53, 1438 (1965).

APPENDIX A
PUBLICATIONS

The following is an abstract of a paper describing work performed on this contract. This paper was delivered at the IEEE Ultrasonics Symposium in New York on September 26, 1968.

EFFECT OF MgO DOPING ON THE ACOUSTIC WAVE ATTENUATION IN $LiNbO_3$ and $LiTaO_3$*

J. C. Worley, A. B. Smith, M. Kestigian, and R. W. Kedzie †
Sperry Rand Research Center
Sudbury, Massachusetts

MgO has been added in varying amounts to the melts of Czochralski-grown single crystals of $LiNbO_3$ and $LiTaO_3$. The effects of this impurity on the longitudinal acoustic wave attenuation at 2.75 GHz have been studied by means of the pulse-echo technique. The attenuation was studied as a function of temperature between 4^o and 250^oK. Measurements have shown that the Mg has altered the temperature dependent part of the attenuation and possibly also affected the residual attenuation observed at low temperatures.

---

* Supported in part by the U. S. Air Force Material Laboratory, Wright-Patterson AFB under contract No. F33615-68-C-1099 and by the National Aeronautics and Space Administration under contract No. NAS 12-571.

† Now employed at Ventron, Magnion, Inc., Burlington, Massachusetts.

APPENDIX B
NEW TECHNOLOGY DISCLOSURE

The following is a copy of the New Technology Disclosure covering the research described in this Final Report.

EFFECT OF MgO DOPING IN REDUCING ACOUSTIC WAVE ATTENUATION IN $LiNbO_3$ and $LiTaO_3$ CRYSTALS

SUMMARY

Because of their low acoustic loss, a number of single crystal insulating materials, such as YAG, ruby, sapphire, $LiNbO_3$ and $LiTaO_3$, have found application in microwave acoustic delay lines[1] and in elasto-optic signal processing devices.[2] It is of great importance to the practical utilization of these devices that the acoustic loss in the material be low. We have developed a method of reducing the acoustic loss in two of these single crystal materials. The two materials in question, $LiTaO_3$ and $LiNbO_3$, are ferroelectrics whose growth procedures have been reported in the literature.[3] We have modified these procedures by adding MgO to the melt while the crystal is being grown. We find that this addition results in the growth of more perfect crystals exhibiting lower acoustic attenuation.

(1) During the growth of single crystal materials, crystal imperfections may develop which will lead to a temperature-independent attenuation of acoustic waves. These imperfections may take the form of impurities, strains, or lattice site vacancies. Thus when measurements are made at a low temperature, the amount of attenuation measured will serve as a gauge as to the quality of the crystal structure. In order to study this mechanism, single crystals of $LiNbO_3$ and $LiTaO_3$ were grown from melts having different stoichiometries and different amounts of MgO added to the melt. Briefly, the result of these experiments was that the addition of MgO served to lower the temperature-independent portion of the attenuation. (The detailed results are presented in the semi-annual progress report on Contract No. NAS 12-571.)

(2) In addition to the temperature-independent term just discussed, the attenuation observed in single crystal materials at room temperature includes a temperature-dependent portion which is caused by the interaction of the sound waves with thermal phonons. Recent tentative results indicate that this temperature-dependent portion of the attenuation in $LiNbO_3$ and $LiTaO_3$ is also reduced by MgO doping.

(3) There are several possible explanations for the improvement in acoustic quality which results when MgO is added to $LiNbO_3$ or $LiTaO_3$ melts. First of all, the addition of small amounts of an impurity ion (such as magnesium) lowers the melting point of the $LiNbO_3$ or $LiTaO_3$. A lower temperature results in less thermal strain in the single crystal. The use of a lower temperature minimizes thermal decomposition (loss of oxygen), thereby also resulting in obtaining a more stoichiometric single crystal.

(4) A second possible advantage which results from adding magnesium oxide to a melt of $LiNbO_3$ or $LiTaO_3$ is related to the condition of the melt itself. The melt becomes more fluid (less viscous) upon the addition of MgO. A more fluid melt enhances the movement of ions and should result in obtaining a more homogeneous single crystal.

(5) The third possible advantage in adding magnesium oxide to a $LiNbO_3$ or $LiTaO_3$ melt involves the filling of vacancies in the lattice caused by the presence of reduced niobium. This process could take place in the liquid phase, single crystal, or both. The formula $Li_{(1-x)}Mg_{(x)}Nb^{5+}_{(1-x)}Nb^{4+}_{(x)}O_3$ would apply. The presence of divalent magnesium would fill A-type vacancies and, by charge compensation with equal amounts of any reduced niobium that is present, prevent oxygen vacancies.

(6) Although chemical analysis has been shown that Mg ions do go into the grown crystal (see 10th and 11th monthly progress reports for Contract NAS-12-571), it is not yet clear whether the improvement in acoustic quality is due to charge compensation according to the above formula or whether it is due to one or more of the other possible mechanisms mentioned above. No matter what mechanism is involved, it does seem clear from our acoustic measurements that MgO-doping does result in a more perfect crystal. The MgO doping techniques should therefore also be valuable in preparing $LiNbO_3$ and $LiTaO_3$ for non-acoustic application such as for use in electro-optic devices.[2]

References

1. R. W. Damon, IEEE Spectrum 4, 87 (June, 1967).

2. E. G. Spencer, P. V. Lenzo, and A. A. Ballman, Proc. IEEE 55, 2074 (1967).

3. S. A. Fedulov, Z. I. Shapiro, P. B. Ladyzhinskii, Soviet Physics-Crystallography 10, 218 (1965); A. A. Ballman, J. Am. Ceram. Soc. 48, 112 (1965); K. Nassau, H. J. Levinstein, G. M. Loiacono, J. Phys. Chem. Solids 27, 983 (1966).